

# EXPLORING STRUCTURAL SPARSITY IN NEURAL IMAGE COMPRESSION

Shanzhi Yin<sup>1</sup>, Chao Li<sup>1</sup>, Wen Tan<sup>1</sup>, Youneng Bao<sup>1</sup>, Yongsheng Liang<sup>1</sup>, Wei Liu<sup>2</sup>

<sup>1</sup>Harbin Institute of Technology, Shenzhen

<sup>2</sup>PengCheng Laboratory

## ABSTRACT

Neural image compression have reached or out-performed traditional methods (such as JPEG, BPG, WebP). However, their sophisticated network structures with cascaded convolution layers bring heavy computational burden for practical deployment. In this paper, we explore the structural sparsity in neural image compression network to obtain real-time acceleration without any specialized hardware design or algorithm. We propose a simple plug-in adaptive binary channel masking(ABCM) to judge the importance of each convolution channel and introduce sparsity during training. During inference, the unimportant channels are pruned to obtain slimmer network and less computation. We implement our method into three neural image compression networks with different entropy models to verify its effectiveness and generalization, the experiment results show that up to  $7\times$  computation reduction and  $3\times$  acceleration can be achieved with negligible performance drop.

**Index Terms**— neural image compression, structural sparsity, channel pruning

## 1. INTRODUCTION

Image compression is an essential and fundamental research topic in signal processing and computer vision. It minimizes the required bits for image coding and reconstruction errors for image decoding at the same time. Recently, neural image compression networks have shown great potential to boost the Rate-Distortion optimization and achieved state-of-the-art performance compared to traditional methods [1–4]. However, these advanced networks are commonly based on complex convolution calculations. Their model complexity can reach more than 50G FLOPs [5], which brings heavy computational overhead for practical hardware deployment and is unfriendly to circumstances like portable electrical devices or edge computing.

To simplify the network structure or reduce the computation of convolution neural network, many researchers have developed network sparsification or dynamic inference techniques. BN parameters [6] and global probabilistic constraint [7] are utilized to prune ineffective structures. Stochastic sampling [8] and channel-dimension correlation [9] are used to judge the important area of current feature maps

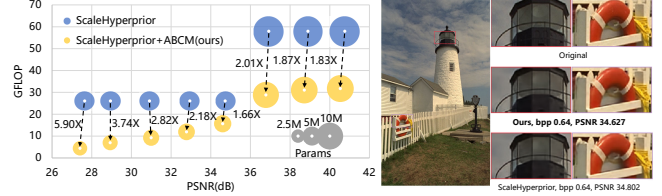


**Fig. 1.** Calculation (up to  $5.9\times$ ) and parameters (up to  $1.7\times$ ) saving on ABCMs embedded ScaleHyperprior models of 8 different quality while performance drop is negligible(left); Our method shows no obvious visual qualitative degradation on the reconstructed image(right).

and implement spatially dynamic inference. However, these methods either lack implementation on image compression task or need specialized hardware programming to achieve real-time acceleration.

In the meantime, sparsity in neural image compression remains an open and less researched problem. Some researchers only focus on the simplification of the neural image decoder with regulation technique [10], multi-branch module [11], or introduce complicated training algorithm [12] with slimmable network [?]. In our previous work [14], we obtain spatial-dimension sparse feature map of NIC models in a simple but effective way, but it needs dynamic convolution and is accordingly unfriendly to real-time acceleration. On the other hand, channel-dimension sparsity can be leveraged to obtain slimmer network structure and maintain static inference, which would be practical for direct hardware acceleration.

To get a slimmer network structure explicitly, we first investigated the channel redundancy in a trained neural image compression(NIC) model. As discussed in [15], the importance of different channels in NIC models varies, removing each of them can result in different reconstruction results. In our experiments, we search layer by layer in main encoder of a trained ScaleHyperprior model [16]. In each layer, we iteratively search and prune one channel that causes the minimum PSNR drop of reconstruction until no channel can be pruned without PSNR drop larger than a certain threshold. Then, we move to the next layer. The layers are searched from input end to the latent end and from decoder-side to encoder-side on each end, corresponding to their potential influence to the re-

construction quality. We set the maximum PSNR drop threshold to different values and see the corresponding pruning ratio that the trained model can achieve. The results in Figure.2 shows that a relatively small PSNR drop value like 1% can only allow a small pruning ratio of no more than 5%, while a pruning ratio of nearly 50% can lead to unacceptable performance drop of more than 10%.

Figure.2 indicates that structural channel sparsity is insufficient in a trained NIC model and needs to be introduced during training procedure. This inspires us to propose adaptive binary channel masking(ABCM) as shown in Fig.3. We use a learnable vector to automatically judge the importance of every convolution output channels. By gating the learnable vector, we can obtain a binary channel-dimension mask, which is then masked on the each output channel to set the unimportant channels to zero. By doing so, we introduce structural sparsity during the training procedure and force the network to gather useful information to important channels decided by ABCM as much as possible. During inference, the zeroed channels are pruned to get slimmer network structure and real-time acceleration subsequently.

We implement our method on three NIC models in a plug-in manner and conduct comprehensive experiments to prove the effectiveness of our method. The effectiveness on Scale-Hyperprior model shown in Fig.1. There is no obvious performance degradation on the reconstructed image, while the parameter and computation saving is quite impressive.

As far as we know, this may be the first work exploring the structural sparsity in neural image compression for real-time inference acceleration. Our contribution are summarized as followed:

- We propose a simple but effective ABCM method that can judge the importance of convolution channels and introduce sparsity during training procedure.
- We implement our ABCM in a plug-in manner and explore the structural sparsity in NIC models to achieve real-time inference acceleration.
- Comprehensive experiment results show that up to  $7\times$  computation reduction and  $3\times$  acceleration can be achieved with negligible performance drop.

## 2. PROPOSED METHOD

### 2.1. Adaptive binary channel masking

In [14], we obtain sparse feature map from NIC convolution output by spatial-wisely judging the significance of each element and zero unimportant locations. In this work ,we focus on the importance of different convolution channels, which is adaptively learned by ABCMs during the training procedure.

As shown in Fig.3, we denote a learnable important vector as  $\alpha$ , which is supposed to automatically judge the influence of each channel to the model performance during the training procedure. Then, the importance vector is gated by a simple

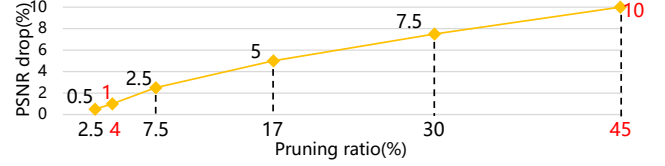


Fig. 2. PSNR drop vs. pruning ratio on trained model

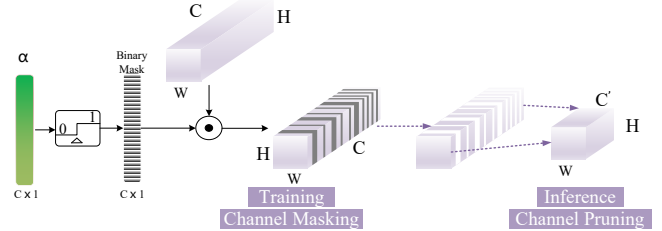


Fig. 3. Proposed adaptive binary channel masking

gating function to obtain a binary channel mask, the gating function can be denoted as:

$$gt(\alpha) = \begin{cases} 1 & \text{if } \alpha \geq 0, \\ 0 & \text{if otherwise,} \end{cases} \quad (1)$$

For this gating function is not differentiable, Sigmoid function  $\sigma(\alpha) = \frac{1}{1+e^{-\epsilon\alpha}}$  is used to replace it during the training process [9]. If we denote the output feature map of convolution layer as  $x$ , ABCM module can set the unimportant channels to zero and its output can be denoted as:

$$x_{mask} = x \odot gt(\alpha) \quad (2)$$

in which  $\odot$  denotes the channel-wise product and  $x_{mask}$  is the channel-dimension sparse feature map. During inference, these zeroed channels in every layer are pruned to get a slimmer network structure with parameters only from effective channels. As the computation of convolution operation is related to the number of its input and output channels, faster inference can be realized with slimmer network.

It should be noted that, during inference, ABCM modules are only used to guide the network pruning and are not used in the consequent slimmer network. The function of ABCM is two-fold: firstly, it introduces sparsity by setting certain channels to zero and forces the network to minimize the effectiveness of these channels during training, so that the original performance of the models can be reserved as much as possible; secondly, by using binary channel mask to introduce sparsity during training, the performance of slimmer model can maintain the same before and after the channel pruning.

### 2.2. Implementation and optimization

To illustrate the effectiveness of our method, we implement ABCM into three existing NIC models [1, 16, 17] with different entropy models, denoted as Factorizedprior model,

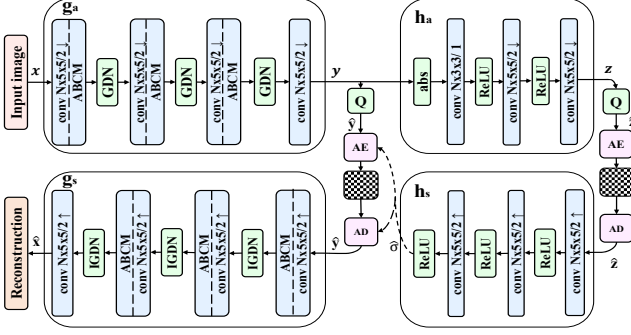


Fig. 4. Implementation on ScaleHyperprior model

ScaleHyperprior model, JointAutoregressive model respectively. In this section, we use ScaleHyperprior model as an example to explain the implement details and optimization formulation of our method.

As shown in Fig.4, we plug totally 6 ABCM modules after convolution layers. The last layer of the main encoder and main decoder are unchanged to maintain the channel number of the network input and entropy coding. Besides, the hyper codec remains unchanged, because we notice that the hyper parameters are significant for keeping an accurate entropy model. If we introduce sparsity in hyper codec, the computational saving cannot compensate for the corresponding performance degradation.

After adopting our method into the original NIC models, it needs to be trained in a end-to-end manner. Similar to most image compression problem, two loss terms rate  $R$  and distortion  $D$  need to be optimized. As the actual arithmetic coding is bypassed [17], the rate term is given by the cross entropy of the estimated distribution of  $y$  and the its actual distribution:

$$R(\hat{y}; \theta, \phi) = \mathbb{E}_{\hat{y} \sim p_y} \{ \log_2 q_y[Q(y)] \} \quad (3)$$

in which,  $\theta, \phi$  denote the parameters of codecs and ABCM modules respectively,  $Q$  represents the quantization process,  $p$  and  $q$  are actual and predicted distribution of image data respectively. In our work, the distortion between the input image and reconstructed image is the mean square error(mse) measured on the test set:

$$D(x, \hat{x}; \theta, \phi) = \mathbb{E}_{x \sim p_x} [\|x - \hat{x}\|^2] \quad (4)$$

Besides, we set a additional sparsity regulation term based on our ABCM modules to ensure the channel-dimension sparsity during the training and achieve the comprehensive trade-off between rate, distortion and sparsity. As discussed in section.2, we denote the importance vector in the  $i$  th ABCM modules as  $\alpha_i$ , gating function as  $gt$ , the corresponding sparsity term  $s_i$  can be expressed as:

$$s_i = \frac{\|gt(\alpha_i)\|_1}{C_i} \quad (5)$$

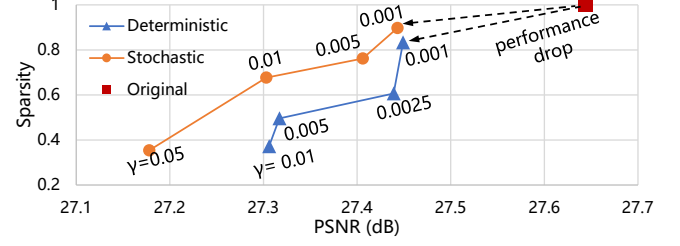


Fig. 5. Ablation study on mask generation and sparsity regulation term, sparsity denotes the ratio of effective channels.

in which,  $\|\cdot\|_1$  denotes the L1-norm and  $C_i$  denotes the channel number of ABCM module. The final optimization problem with  $n$  ABCM modules can be formulated as:

$$\operatorname{argmin}_{\theta, \phi} [R + \lambda D + \gamma \frac{1}{n} \sum_{i=1}^n s_i] \quad (6)$$

in which,  $R, D, s_i$  are defined by equation(3)(4)(5) respectively,  $\lambda$  and  $\gamma$  are hyper parameters to control the trade-off between rate, distortion and sparsity. When tuning these two hyper parameters, a proper level of sparsity can be achieved with acceptable or even negligible performance degradation.

### 3. EXPERIMENTS

We use CLIC dataset<sup>1</sup> to train our models for 100 epochs. We adopted CompressAI [18] re-implantation of NIC models and followed most of their training settings, except that we reduce learning rate by 0.5 only once after 64 epochs, i.e. approximately 1 million steps. All trained models are evaluated on Kodak dataset<sup>2</sup>.

#### 3.1. Ablation study

Before we implement our method, we did ablation study on two aspects, using ScaleHyperprior quality=1 model.

**Mask generation.** As several work has illustrated the effectiveness of treating network sparsity as a probabilistic event [7, 19], the importance vector can be either a learnable parameter itself, or a Bernoulli sampling from a  $2 \times C$  learnable parameter with reparameterization trick [20]. We denote these two methods as Deterministic and Stochastic.

**Sparsity regulation term.** The hyper parameter  $\gamma$  controls the trade-off between network sparsity and performance. Choosing a appropriate  $\gamma$  can contribute to the comprehensive optimization in equation(6).

As we tune the value of  $\gamma$ , the bpp remains 0.14, while the PSNR( $10 \log_{10} \frac{255^2}{mse}$ ) and average sparsity of all ABCM modules on test set are shown in Fig.5. We can see that the deterministic mask generation can achieve relatively higher

<sup>1</sup>The CLIC Dataset can be accessed at <http://compression.cc/>

<sup>2</sup>The Kodak Dataset can be accessed at <http://r0k.us/graphics/kodak/>

**Table 1.** The PSNR, Parameters and FLOP reduction of models on Kodak set

Model	Reduction	Quality							
		1	2	3	4	5	6	7	8
Factorizedprior	PSNR(%)	0.739	0.391	0.990	0.552	0.440	0.728	0.298	0.223
	Params	<b>5.63</b> $\times$	<b>3.80</b> $\times$	<b>2.81</b> $\times$	<b>2.13</b> $\times$	<b>1.70</b> $\times$	<b>1.60</b> $\times$	<b>1.40</b> $\times$	<b>1.31</b> $\times$
	FLOP (with ABCMs)	<b>7.17</b> $\times$	<b>4.35</b> $\times$	<b>3.01</b> $\times$	<b>2.17</b> $\times$	<b>1.61</b> $\times$	<b>2.13</b> $\times$	<b>1.83</b> $\times$	<b>1.72</b> $\times$
ScaleHyperprior	PSNR(%)	0.857	0.052	0	0.504	0.306	0.393	0.473	0.552
	Params	<b>1.73</b> $\times$	<b>1.60</b> $\times$	<b>1.39</b> $\times$	<b>1.30</b> $\times$	<b>1.22</b> $\times$	<b>1.25</b> $\times$	<b>1.19</b> $\times$	<b>1.17</b> $\times$
	FLOP (with ECGs [14])	2.54 $\times$	2.86 $\times$	2.60 $\times$	2.54 $\times$	2.54 $\times$	2.07 $\times$	2.14 $\times$	2.03 $\times$
JointAutoregressive	FLOP (with ABCMs)	<b>5.90</b> $\times$	<b>3.74</b> $\times$	<b>2.82</b> $\times$	<b>2.18</b> $\times$	<b>1.66</b> $\times$	<b>2.01</b> $\times$	<b>1.87</b> $\times$	<b>1.83</b> $\times$
	PSNR(%)	1.17	0.963	0.553	0.662	0.402	0.601	0.667	0.451
	Params	<b>1.49</b> $\times$	<b>1.43</b> $\times$	<b>1.35</b> $\times$	<b>1.30</b> $\times$	<b>1.13</b> $\times$	<b>1.09</b> $\times$	<b>1.08</b> $\times$	<b>1.05</b> $\times$
JointAutoregressive	FLOP (with ECGs [14])	2.34 $\times$	2.50 $\times$	2.56 $\times$	2.68 $\times$	2.33 $\times$	2.12 $\times$	2.12 $\times$	2.24 $\times$
	FLOP (with ABCMs)	<b>6.39</b> $\times$	<b>4.77</b> $\times$	<b>3.76</b> $\times$	<b>2.80</b> $\times$	<b>2.24</b> $\times$	<b>1.89</b> $\times$	<b>1.78</b> $\times$	<b>1.53</b> $\times$

**Table 2.** The real-time acceleration for 768 $\times$ 512 input image on different devices

Model	Devices	Quality							
		1	2	3	4	5	6	7	8
Factorizedprior	Intel Xeon Gold 5118	3.40 $\times$	2.67 $\times$	2.07 $\times$	1.91 $\times$	1.39 $\times$	1.65 $\times$	1.46 $\times$	1.35 $\times$
	NVIDIA Tesla V100	1.30 $\times$	1.28 $\times$	1.16 $\times$	1.13 $\times$	1.09 $\times$	1.78 $\times$	1.53 $\times$	1.50 $\times$
ScaleHyperprior	Intel Xeon Gold 5118	3.12 $\times$	2.19 $\times$	1.96 $\times$	1.90 $\times$	1.38 $\times$	1.45 $\times$	1.39 $\times$	1.37 $\times$
	NVIDIA Tesla V100	1.31 $\times$	1.29 $\times$	1.18 $\times$	1.14 $\times$	1.10 $\times$	1.75 $\times$	1.61 $\times$	1.58 $\times$
JointAutoregressive	Intel Xeon Gold 5118	2.83 $\times$	2.60 $\times$	1.99 $\times$	1.62 $\times$	1.45 $\times$	1.40 $\times$	1.41 $\times$	1.26 $\times$
	NVIDIA Tesla V100	2.33 $\times$	2.12 $\times$	2.08 $\times$	1.91 $\times$	1.81 $\times$	1.57 $\times$	1.53 $\times$	1.19 $\times$

sparsity with less performance drop. To maintain acceptable performance drop and obtain network sparsity as much as possible, we choose deterministic mask generation and set  $\gamma = 0.01$  in subsequent experiments.

### 3.2. R-D and efficiency performance

We implement our method in three NIC models to build efficient models with promising saving in both parameters and computation. When embedded with ABCMs, we observe that the bit-rate of our models fluctuate around their original ones. For fair comparison, we fine-tuned  $\lambda$  and trained one more epoch so that our bit-rates are the same (accurate to two decimal places) as their original counterparts.

Table.1 shows the parameters and FLOP reduction of efficient models obtained by ABCMs guided pruning. We can see that up to 5.63 $\times$ , 1.73 $\times$ , 1.49 $\times$  parameters saving and up to 7.17 $\times$ , 5.90 $\times$ , 6.39 $\times$  FLOP reduction can be achieved in three models with PSNR drop around 0.5%. It should be noted that, such efficiency is achieved under hyperparameter  $\gamma = 0.01$ , when tuning its value, the trade-off between performance and efficiency can be arbitrary.

The results show that channel redundancy commonly exist in neural image compression network. Under the same channel number configuration, lower the quality is (smaller the hyperparameter  $\lambda$  is), sparser the network can be. Even with the highest quality model, the FLOP can be reduced by nearly 2 times. Compared to ECG modules in [14], our

ABCMs perform much better in low quality model and can be directly utilized for real-time acceleration.

To measure the real-time acceleration of efficient models on both CPU and GPU, we chose Kodim.19 in Kodak set as the input image. Considering the warm-up and multi-threading of the devices, we take ten rounds of inference as warm-up and take another ten rounds as formal tests, then record the average duration of each round.

Table.2 shows the real-time acceleration (excluding data loading/writing and arithmetic coding) on a NVIDIA Tesla V100 GPU and Intel(R) Xeon(R) Gold 5118 CPU, which corresponds to the FLOP reduction in Table.1. We can see that up to 3.40 $\times$ , 3.12 $\times$ , 2.83 $\times$  real-time CPU acceleration and up to 1.30 $\times$ , 1.31 $\times$ , 2.33 $\times$  real-time GPU acceleration can be achieved in three models. Such acceleration would be more obvious and beneficial on big data or continuous processing.

## 4. CONCLUSION

In this paper, we explore the channel-dimension structural sparsity in existing neural image compression models to obtain real-time acceleration. We implementing our plug-in adaptive binary channel masking in three different NIC models to verify its effectiveness and generalization. Comprehensive experiment results show that 1.2-3.4 $\times$  inference acceleration and 1.5-7.1 $\times$  parameter saving can be achieved with less than 1% performance drop. Potential future work includes better joint optimization, complexity-rate control.

## 5. REFERENCES

- [1] David Minnen, Johannes Ballé, and George D Toderici, “Joint autoregressive and hierarchical priors for learned image compression,” *Advances in Neural Information Processing Systems*, vol. 31, pp. 10771–10780, 2018.
- [2] Zhengxue Cheng, Heming Sun, Masaru Takeuchi, and Jiro Katto, “Learned image compression with discretized gaussian mixture likelihoods and attention modules,” in *Proceedings of the IEEE/CVF Conference on Computer Vision and Pattern Recognition*, 2020, pp. 7939–7948.
- [3] Tong Chen, Haojie Liu, Zhan Ma, Qiu Shen, Xun Cao, and Yao Wang, “End-to-end learnt image compression via non-local attention optimization and improved context modeling,” *IEEE Transactions on Image Processing*, vol. 30, pp. 3179–3191, 2021.
- [4] Ze Cui, Jing Wang, Shangyin Gao, Tiansheng Guo, Yihui Feng, and Bo Bai, “Asymmetric gained deep image compression with continuous rate adaptation,” in *Proceedings of the IEEE/CVF Conference on Computer Vision and Pattern Recognition*, 2021, pp. 10532–10541.
- [5] Zhengxue Cheng, Heming Sun, Masaru Takeuchi, and Jiro Katto, “Deep residual learning for image compression,” in *CVPR Workshops*, 2019, p. 0.
- [6] Zhuang Liu, Jianguo Li, Zhiqiang Shen, Gao Huang, Shoumeng Yan, and Changshui Zhang, “Learning efficient convolutional networks through network slimming,” in *Proceedings of the IEEE international conference on computer vision*, 2017, pp. 2736–2744.
- [7] Xiao Zhou, Weizhong Zhang, Hang Xu, and Tong Zhang, “Effective sparsification of neural networks with global sparsity constraint,” in *Proceedings of the IEEE/CVF Conference on Computer Vision and Pattern Recognition*, 2021, pp. 3599–3608.
- [8] Zhenda Xie, Zheng Zhang, Xizhou Zhu, Gao Huang, and Stephen Lin, “Spatially adaptive inference with stochastic feature sampling and interpolation,” in *European Conference on Computer Vision*. Springer, 2020, pp. 531–548.
- [9] Weizhe Hua, Yuan Zhou, Christopher De Sa, Zhiru Zhang, and G Edward Suh, “Channel gating neural networks,” in *Proceedings of the 33rd International Conference on Neural Information Processing Systems*, 2019, pp. 1886–1896.
- [10] Nick Johnston, Elad Eban, Ariel Gordon, and Johannes Ballé, “Computationally efficient neural image compression,” *arXiv preprint arXiv:1912.08771*, 2019.
- [11] Jinyang Guo, Dong Xu, and Guo Lu, “Cbanet: Towards complexity and bitrate adaptive deep image compression using a single network,” *arXiv preprint arXiv:2105.12386*, 2021.
- [12] Fei Yang, Luis Herranz, Yongmei Cheng, and Mikhail G Mozerov, “Slimmable compressive autoencoders for practical neural image compression,” in *Proceedings of the IEEE/CVF Conference on Computer Vision and Pattern Recognition*, 2021, pp. 4998–5007.
- [13] Changlin Li, Guangrun Wang, Bing Wang, Xiaodan Liang, Zhihui Li, and Xiaojun Chang, “Dynamic slimmable network,” in *Proceedings of the IEEE/CVF Conference on Computer Vision and Pattern Recognition*, 2021, pp. 8607–8617.
- [14] Shanzhi Yin, Chao Li, Youneng Bao, and Yongsheng Liang, “Universal efficient variable-rate neural image compression,” 2021.
- [15] Zhisheng Zhong, Hiroaki Akutsu, and Kiyoharu Aizawa, “Channel-level variable quantization network for deep image compression,” in *Proceedings of the Twenty-Ninth International Joint Conference on Artificial Intelligence, IJCAI-20*, Christian Bessiere, Ed. 7 2020, pp. 467–473, International Joint Conferences on Artificial Intelligence Organization, Main track.
- [16] Johannes Ballé, David Minnen, Saurabh Singh, Sung Jin Hwang, and Nick Johnston, “Variational image compression with a scale hyperprior,” *arXiv preprint arXiv:1802.01436*, 2018.
- [17] Johannes Ballé, Valero Laparra, and Eero P. Simoncelli, “Density modeling of images using a generalized normalization transformation,” in *4th International Conference on Learning Representations, ICLR 2016 - Conference Track Proceedings*, nov 2016.
- [18] Jean Bégaint, Fabien Racapé, Simon Feltman, and Akshay Pushparaja, “Compressai: a pytorch library and evaluation platform for end-to-end compression research,” *arXiv preprint arXiv:2011.03029*, 2020.
- [19] Longguang Wang, Xiaoyu Dong, Yingqian Wang, Xinyi Ying, Zaiping Lin, Wei An, and Yulan Guo, “Exploring sparsity in image super-resolution for efficient inference,” in *Proceedings of the IEEE/CVF Conference on Computer Vision and Pattern Recognition*, 2021, pp. 4917–4926.
- [20] Eric Jang, Shixiang Gu, and Ben Poole, “Categorical reparameterization with gumbel-softmax,” in *5th International Conference on Learning Representations, ICLR 2017 - Conference Track Proceedings*, 2017.

## 6. APPENDIX

**Table 3.** Detailed channel configuration of efficient models

ScaleHyperprior																					
Module	Layer	channel (low)		channel (high)		(Q1)		(Q2)		(Q3)		(Q4)		(Q5)		(Q6)		(Q7)		(Q8)	
		in	out	in	out	in	out	in	out	in	out	in	out	in	out	in	out	in	out	in	out
ga	conv	3	128	3	192	3	30	3	38	3	50	3	66	3	95	3	111	3	128	3	133
	GDN	128	128	192	192	30	30	38	38	50	50	66	66	95	95	111	111	128	128	133	133
	conv	128	128	192	192	30	39	38	48	50	71	66	90	95	107	111	146	128	166	133	176
	GDN	128	128	192	192	39	39	48	48	71	71	90	90	107	107	146	146	166	166	176	176
	conv	128	128	192	192	39	48	48	63	71	86	90	94	107	88	146	144	166	166	176	174
	GDN	128	128	192	192	48	48	63	63	86	86	94	94	88	88	144	144	166	166	174	174
conv	128	192	192	320	48	192	63	192	63	86	192	94	192	88	192	144	320	166	320	174	320
gs	conv	192	128	320	192	192	81	192	88	192	117	192	117	126	126	320	191	320	189	320	178
	GDN	128	128	192	192	81	81	88	88	117	117	117	117	126	126	191	191	189	189	178	178
	conv	128	128	192	192	81	41	88	57	117	63	117	77	126	89	191	118	189	119	178	128
	GDN	128	128	192	192	41	41	57	57	63	63	77	77	89	89	118	118	119	119	128	128
	conv	128	128	192	192	41	40	57	62	63	70	77	80	94	94	118	124	119	128	128	121
	GDN	128	128	192	192	40	40	62	62	70	70	80	80	94	94	124	124	128	128	121	121
conv	128	3	192	3	40	3	62	3	70	3	80	3	94	3	124	3	128	3	121	3	
JointAutoregressive																					
Module	Layer	channel (low)		channel (high)		(Q1)		(Q2)		(Q3)		(Q4)		(Q5)		(Q6)		(Q7)		(Q8)	
		in	out	in	out	in	out	in	out	in	out	in	out	in	out	in	out	in	out	in	out
ga	conv	3	192	3	192	3	30	3	46	3	61	3	80	3	81	3	117	3	130	3	149
	GDN	192	192	192	192	30	30	46	46	61	61	80	80	81	81	117	117	130	130	149	149
	conv	192	192	192	192	30	66	46	73	61	92	80	122	81	140	117	155	130	174	149	180
	GDN	192	192	192	192	66	66	73	73	92	92	122	122	140	140	155	155	174	174	180	180
	conv	192	192	192	192	66	56	73	73	92	116	122	99	140	144	155	165	174	178	180	190
	GDN	192	192	192	192	56	56	73	73	116	116	99	99	144	144	165	165	178	178	190	190
conv	192	192	192	320	56	192	73	192	116	192	99	192	144	320	165	320	178	320	190	320	
gs	conv	192	192	320	192	192	101	192	126	192	141	192	163	320	168	320	182	320	176	320	175
	GDN	192	192	192	192	101	101	126	126	141	141	163	163	168	168	182	182	176	176	175	175
	conv	192	192	192	192	101	49	126	66	141	78	163	93	168	94	182	107	176	127	175	143
	GDN	192	192	192	192	49	49	66	66	78	78	93	93	94	94	107	107	127	127	143	143
	conv	192	192	192	192	49	59	66	71	78	82	93	105	94	112	107	121	127	107	143	126
	GDN	192	192	192	192	59	59	71	71	82	82	105	105	112	112	121	121	107	107	126	126
conv	192	3	192	3	59	3	71	3	82	3	105	3	112	3	121	3	107	3	126	3	
Factorizedprior																					
Module	Layer	channel (low)		channel (high)		(Q1)		(Q2)		(Q3)		(Q4)		(Q5)		(Q6)		(Q7)		(Q8)	
		in	out	in	out	in	out	in	out	in	out	in	out	in	out	in	out	in	out	in	out
ga	conv	3	128	3	192	3	35	3	44	3	58	3	75	3	93	3	93	3	115	3	133
	GDN	128	128	192	192	35	35	44	44	58	58	75	75	93	93	93	93	115	115	133	133
	conv	128	128	192	192	35	40	44	56	58	75	75	93	93	108	93	151	115	173	133	177
	GDN	128	128	192	192	40	40	56	56	75	75	93	93	108	108	151	151	173	173	177	177
	conv	128	128	192	192	40	33	56	44	75	55	93	67	108	79	151	134	173	156	177	172
	GDN	128	128	192	192	33	33	44	44	55	55	67	67	79	79	134	134	156	156	172	172
conv	128	192	192	320	33	128	44	128	55	128	67	128	79	128	134	320	156	320	172	320	
gs	conv	192	128	320	192	128	65	128	85	128	102	128	117	128	127	320	177	320	178	320	179
	GDN	128	128	192	192	65	65	85	85	102	102	117	117	127	127	177	177	178	178	179	179
	conv	128	128	192	192	65	53	85	66	102	72	117	88	127	101	177	120	178	131	179	133
	GDN	128	128	192	192	53	53	66	66	72	72	88	88	101	101	120	120	131	131	133	133
	conv	128	128	192	192	53	34	66	49	72	67	88	77	101	94	120	124	131	131	133	135
	GDN	128	128	192	192	34	34	49	49	67	67	77	77	94	94	124	124	131	131	135	135
conv	128	3	192	3	34	3	49	3	67	3	77	3	94	3	124	3	131	3	135	3	